






Syntheses, crystal structure, and characterization of two Mn(II) CPs based on 4,4'-sulfonyldicarboxylic acid and length modulated bisimidazole ligands

Daofu Liu

To cite this article: Daofu Liu (2015) Syntheses, crystal structure, and characterization of two Mn(II) CPs based on 4,4'-sulfonyldicarboxylic acid and length modulated bisimidazole ligands, Journal of Coordination Chemistry, 68:10, 1655-1663, DOI: [10.1080/00958972.2015.1021344](https://doi.org/10.1080/00958972.2015.1021344)


To link to this article: <http://dx.doi.org/10.1080/00958972.2015.1021344>

 View supplementary material 

 Accepted author version posted online: 02 Mar 2015.
Published online: 16 Mar 2015.

 Submit your article to this journal 

 Article views: 48

 View related articles 

 View Crossmark data 

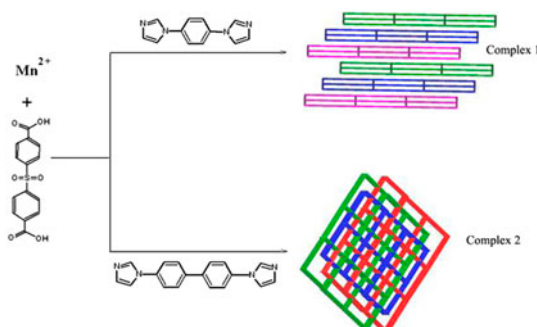
Syntheses, crystal structure, and characterization of two Mn(II) CPs based on 4,4'-sulfonyldicarboxylic acid and length modulated bisimidazole ligands

DAOFU LIU*^{†‡}

[†]Department of Chemistry and Chemical Engineering, Huainan Normal University, Huainan, China

[‡]School of Chemistry & Chemical Engineering, Anhui University, Hefei, China

(Received 20 July 2014; accepted 30 January 2015)



Two new coordination polymers based on imidazole-containing ligands with different spacers, $\{[\text{Mn}(4,4'\text{-sdb})(\text{L}_1)_{0.5}] \cdot 0.5(\text{L}_1)\}_n$ (**1**) and $[\text{Mn}(4,4'\text{-sdb})(\text{L}_2)]_n$ (**2**) [4,4'-H₂sdb = 4,4'-sulfonyldicarboxylic acid, L₁ = 1,4-bis(1-imidazolyl)benzene, and L₂ = 4,4'-bis(1-imidazolyl)biphenylene], have been synthesized under hydrothermal conditions. Complex **1** shows a 2-D layer structure with a sql topological net. Complex **2** features a 3-D framework with CdS topology. In addition, the fluorescent properties of **1** and **2** have been investigated.

Keywords: Mn(II); Crystal structure; Hydrothermal; Luminescence

1. Introduction

The design and construction of coordination polymers (CPs) based on metal ions and multifunctional organic ligands have attracted interest for multifunctional applications in gas and selective molecule adsorption, luminescence, ion exchange, magnetism, and catalysis [1–10] and for intriguing molecular architectures and topological features [11–13]. Self-assembly of CPs mainly depends on combination of several factors, such as the nature

*Email: hnliudf@163.com

of the organic ligands used, versatility of the metal coordination geometry, and various experimental conditions (pH, temperature, etc.) [14–20]. Increasing interest has concentrated on N-donor bridging ligands because it is the most important factor in construction of networks with different dimensionalities. Among various N-donor ligands, imidazole-containing ligands attract attention recently [21–23]. In this article, we explore the effect of the spacer of imidazole-based ligands on the structures of complexes; imidazole-containing ligands with different spacers, 1,4-bis(1-imidazolyl)benzene (L_1), and 4,4'-bis(1-imidazolyl)biphenylene (L_2), were employed to construct CPs. Aromatic dicarboxylates, as multidentate O-donors, are good for self-assembly of CPs because they can provide both structural scaffolding and necessary charge equalization. Two CPs have been synthesized by using 4,4'-H₂sdb and L_1/L_2 under hydrothermal conditions, $\{[\text{Mn}(4,4'\text{-sdb})(L_1)_{0.5}]\cdot 0.5(L_1)\}_n$ (**1**) and $[\text{Mn}(4,4'\text{-sdb})(L_2)]_n$ (**2**). The effect of different N-donor ligands on the resulting frameworks is discussed. In addition, photoluminescence properties of **1** and **2** have also been investigated.

2. Experimental

2.1. General materials and methods

All reagents and solvents were commercially available and used as received. Elemental analyses (C, H, and N) were performed with a VarioEL III Elemental analyzer. Infrared spectra as KBr pellets were recorded with a BRUKER EQUINOX 55 spectrometer from 4000 to 400 cm^{-1} . X-ray powder diffraction (XRPD) measurements were performed on a Bruker D8 diffractometer operated at 40 kV and 40 mA using Cu-K α radiation ($\lambda = 0.15418$ nm). Luminescence spectra for the solid samples were recorded with a Hitachi F-4500 fluorescence spectrophotometer at room temperature.

2.2. Syntheses of complexes

2.2.1. $\{[\text{Mn}(4,4'\text{-sdb})(L_1)_{0.5}]\cdot 0.5(L_1)\}_n$ (1**).** A mixture of $\text{MnCl}_2\cdot 4\text{H}_2\text{O}$ (0.099 g, 0.5 mM), 4,4'-H₂sdb (0.153 g, 0.5 mM), L_1 (0.105 g, 0.5 mM), NaOH (0.04 g, 1 mM), and deionized water (15 mL) was heated at 160 °C for 72 h and then cooled to room temperature. Brown block crystals were obtained and washed with ethanol several times (Yield: 46% based on Mn). Elemental Anal. Calcd (%) for $\text{C}_{26}\text{H}_{18}\text{MnSN}_4\text{O}_6$: C, 54.84; H, 3.19; N, 9.84; S, 5.63. Found: C, 54.85; H, 3.19; N, 9.83; S, 5.64. IR/ cm^{-1} : 1601s, 1522s, 1415s, 1387m, 1227m, 1169m, 1047m, 901m, 844m, 763m.

2.2.2. $[\text{Mn}(4,4'\text{-sdb})(L_2)]_n$ (2**).** Complex **2** was obtained by the same hydrothermal procedure as for preparation of **1** only using L_2 (0.5 mM, 0.143 g) instead of L_1 . Yellow block crystals of **2** were collected in 41% yield based on Mn after washing by ethanol several times. Elemental Anal. Calcd (%) for $\text{C}_{32}\text{H}_{22}\text{MnSN}_4\text{O}_6$: C, 59.54; H, 3.44; N, 8.68; S, 4.97. Found: C, 59.52; H, 3.44; N, 8.69; S, 4.97. IR/ cm^{-1} : 1624s, 1407s, 1339m, 1217w, 1155m, 907m, 876w, 728m.

2.3. X-ray crystallography

Single-crystal X-ray diffraction analyses of **1** and **2** were carried out on a Bruker SMART APEX II CCD diffractometer equipped with graphite monochromated Mo-K α radiation ($\lambda = 0.71073 \text{ \AA}$) by using ω -scan mode. Empirical absorption correction was applied using SADABS [24]. The structures were solved by direct methods and refined by full-matrix least-squares on F^2 using SHELXL 97 [25]. All non-hydrogen atoms were refined anisotropically. Hydrogens were located by geometrically calculations, and their positions and thermal parameters were fixed during the structure refinement. The crystallographic data and experimental details of structural analyses for **1** and **2** are summarized in table 1. Selected bond and angle parameters are listed in table 2.

3. Results and discussion

3.1. Description of the crystal structures

3.1.1. $\{[\text{Mn}(4,4'\text{-sdb})(\text{L}_1)_{0.5}]\cdot 0.5(\text{L}_1)\}_n$ (1**).** Single-crystal X-ray diffraction analysis reveals that **1** consists of dinuclear Mn(II) units symmetrically bridged by four carboxylates. Mn1(II) is five-coordinate with four carboxylate oxygens [Mn–O, ranging from 2.1130(12) to 2.1365(12) \AA] and one nitrogen [Mn(1)–N(1) = 2.1400(12) \AA] to give a square-pyramidal geometry (figure 1). The four carboxylate groups bridge the dinuclear Mn(II) center in *syn-syn* coordination which leads to a paddle wheel secondary building unit (SBU). The Mn \cdots Mn distance within the SBU is 3.141 \AA . In **1**, there exist two types of L₁ molecules, coordinating and not coordinating to manganese. The L₁ coordinating link the 1-D chains

Table 1. Crystallographic data and details of diffraction experiments for **1** and **2**.

	1	2
Formula	C ₂₆ H ₁₈ MnSN ₄ O ₆	C ₃₂ H ₂₂ MnN ₄ O ₆ S
M_r	569.44	645.54
Crystal system	Triclinic	Monoclinic
Space group	<i>P</i> -1	1a
a (\AA)	8.3360(8)	15.4654(7)
b (\AA)	11.9540(12)	10.2339(4)
c (\AA)	13.3580(13)	18.6591(12)
α ($^\circ$)	88.5240(15)	90.000
β ($^\circ$)	75.1750(15)	97.8090(10)
γ ($^\circ$)	70.2510(14)	90.000
V (\AA^3)	1208.4(2)	2925.8(3)
Z	2	4
$F(0\ 0\ 0)$	582	1324
μ (mm^{-1})	0.684	0.575
ρ (g cm^{-3})	1.565	1.465
R_{int}	0.0153	0.028
R^a , wR^b [$I > 2\sigma(I)$]	$R_1 = 0.0285$, $wR_2 = 0.0754$	$R_1 = 0.0314$, $wR_2 = 0.0601$
R^a , wR^b [all data]	$R_1 = 0.0317$, $wR_2 = 0.0781$	$R_1 = 0.0367$, $wR_2 = 0.0616$
Gof	1.028	1.018
Max/min ($e \text{ \AA}^{-3}$)	0.383 and -0.281	0.246 and -0.254

$$^a R = \Sigma(|F_o| - |F_c|) / \Sigma|F_o|$$

$$^b wR = [\Sigma w(|F_o|^2 - |F_c|^2)^2 / \Sigma w(F_o^2)]^{1/2}$$

Table 2. Selected bond lengths (Å) and angles (°) for **1** and **2**.

Complex 1			
Mn(1)–O(1)	2.1199(12)	Mn(1)–O(5) ⁱ	2.1130(12)
Mn(1)–O(2) ⁱⁱⁱ	2.1365(12)	Mn(1)–O(6) ⁱⁱ	2.1171(12)
Mn(1)–N(1)	2.1400(12)		
O(5) ⁱ –Mn(1)–O(6) ⁱⁱ	154.96(6)	O(1)–Mn(1)–N(1)	99.58(5)
O(5) ⁱ –Mn(1)–O(1)	85.79(6)	O(2) ⁱⁱⁱ –Mn(1)–N(1)	105.55(5)
O(6) ⁱⁱ –Mn(1)–O(1)	89.11(6)	O(1)–Mn(1)–O(2) ⁱⁱⁱ	154.81(5)
O(5) ⁱ –Mn(1)–O(2) ⁱⁱⁱ	88.00(6)	O(5) ⁱ –Mn(1)–N(1)	108.26(5)
O(6) ⁱⁱ –Mn(1)–O(2) ⁱⁱⁱ	86.26(6)	O(6) ⁱⁱ –Mn(1)–N(1)	96.75(5)
Complex 2			
Mn(1)–O(1)	2.188(2)	Mn(1)–N(1)	2.156(2)
Mn(1)–O(2)	2.282(2)	Mn(1)–N(4) ⁱⁱ	2.175(2)
Mn(1)–O(5) ⁱ	2.068(2)		
O(5) ⁱ –Mn(1)–N(1)	135.61(9)	O(5) ⁱ –Mn(1)–O(2)	96.79(9)
O(5) ⁱ –Mn(1)–N(4) ⁱⁱ	97.35(9)	N(1)–Mn(1)–O(2)	95.28(8)
N(1)–Mn(1)–N(4) ⁱⁱ	98.06(8)	N(4) ⁱⁱ –Mn(1)–O(2)	143.05(8)
O(5) ⁱ –Mn(1)–O(1)	105.65(10)	N(4) ⁱⁱ –Mn(1)–O(1)	85.27(8)
N(1)–Mn(1)–O(1)	116.92(9)		

Notes: Symmetry codes for **1**: (i) $-x + 2, -y, -z + 1$; (ii) $x, y, z + 1$; (iii) $-x + 2, -y, -z + 2$; for **2**: (i) $x - 1/2, y + 1/2, z + 1/2$; (ii) $x + 1, -y + 1/2, z + 1/2$.

to form a 2-D layer structure and free L_1 fill the voids of the 2-D framework (figure 2). In **1**, the 2-D layers stack with a ABC-sequence along the $[1,2,0]$ direction (figure 3).

3.1.2. $[\text{Mn}(4,4'\text{-sdb})(L_2)]_n$ (2**).** Complex **2** crystallizes in the monoclinic system, space group $1a$. As shown in figure 4, there is one crystallographically independent Mn(II), one 4,4'-sdb and L_2 . Mn(II) has a square pyramidal coordination sphere, which is defined by

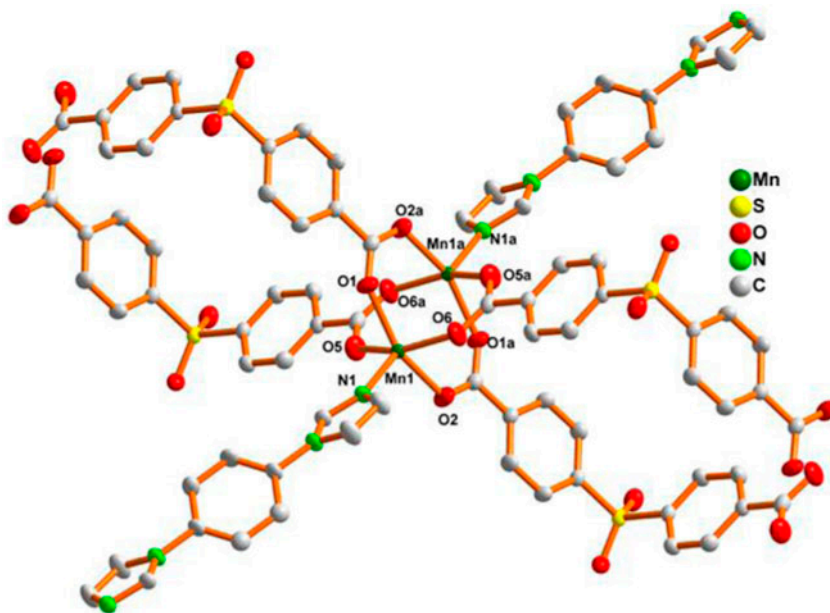


Figure 1. The coordination environment for Mn(II) in **1**. All hydrogens are omitted for clarity.

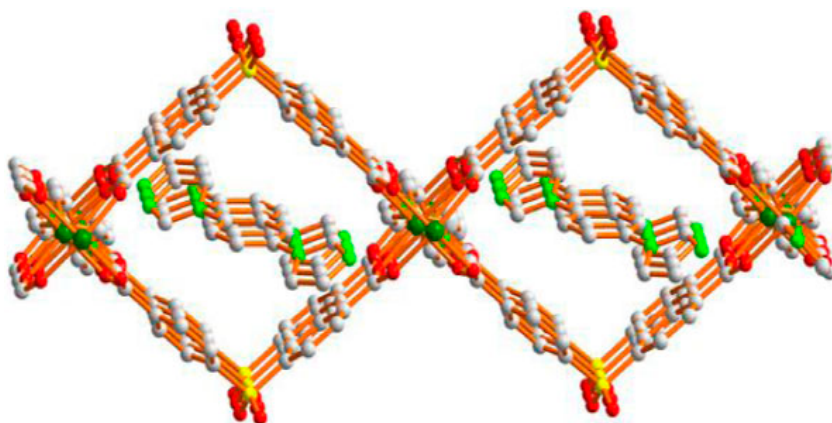


Figure 2. The 2-D framework for **1** and the L_1 of not coordinating to the metals filled the voids.

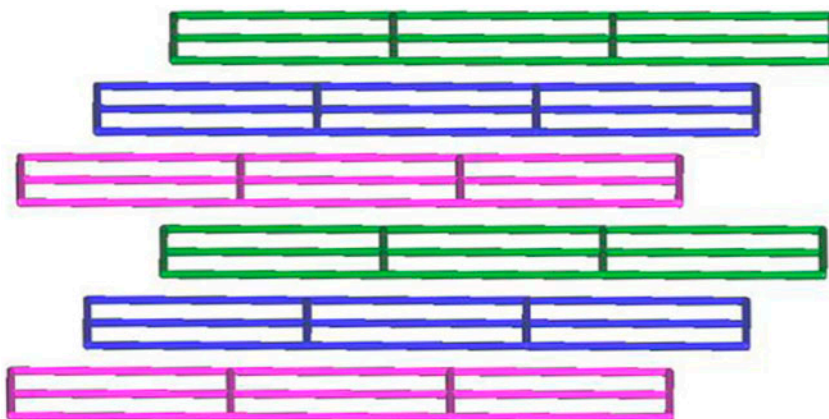


Figure 3. Packing diagram depicting the ABC-type stacks of 2-D sheet in **1**.

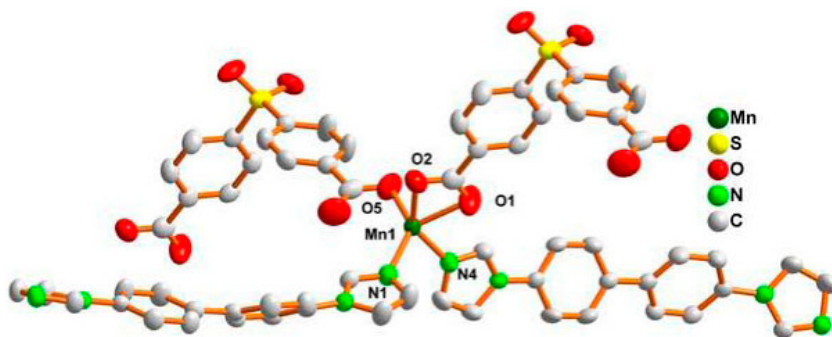


Figure 4. The coordination environment for Mn(II) in **2**. All hydrogens are omitted for clarity.

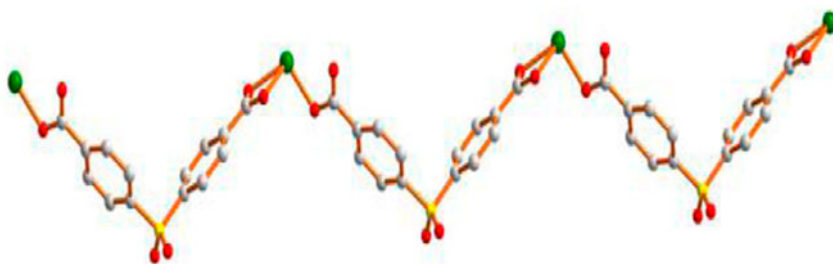


Figure 5. The 1-D chain formed by carboxylate ligands and Mn(II) ions.

three carboxylate oxygens from two different 4,4'-sdb ligands [$\text{Mn}(1)\text{--O}(1) = 2.188(2) \text{ \AA}$, $\text{Mn}(1)\text{--O}(2) = 2.282(2) \text{ \AA}$ and $\text{Mn}(1)\text{--O}(5) = 2.068(2) \text{ \AA}$], and two coordinated nitrogens from two L_2 ligands [$\text{Mn}(1)\text{--N}(1) = 2.156(2) \text{ \AA}$ and $\text{Mn}(1)\text{--N}(4) = 2.175(2) \text{ \AA}$]. The 4,4'-sdb ligands connect Mn(II) ions to form a 1-D chain (figure 5). The L_2 link the 1-D chains with different propagating direction to form a 3-D framework (figure 6).

Better insight into the framework is provided by a topology analysis, reducing multidimensional structures to simple nodes and connection nodes. The Mn(II) ions can be regarded as four-connected nodes and all crystallographical independent ligands act as linkers. Therefore, the whole structure can thus be represented as a CdS topology with the point symbol $(6^5.8)$. Because of the spacious nature of the single network, potential channels in **2** are filled via interpenetration of two independent identical nets, generating a threefold interpenetration framework (figure 7).

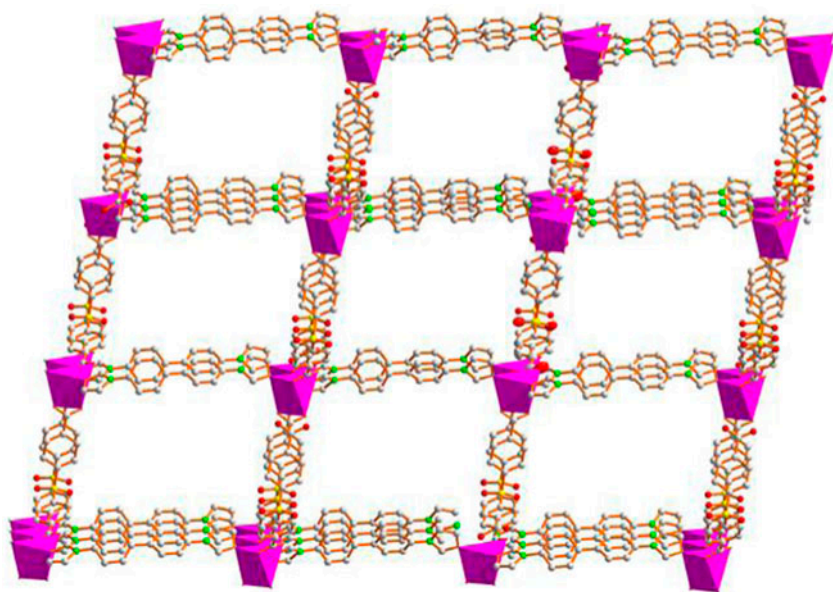


Figure 6. The 3-D framework for **2**.

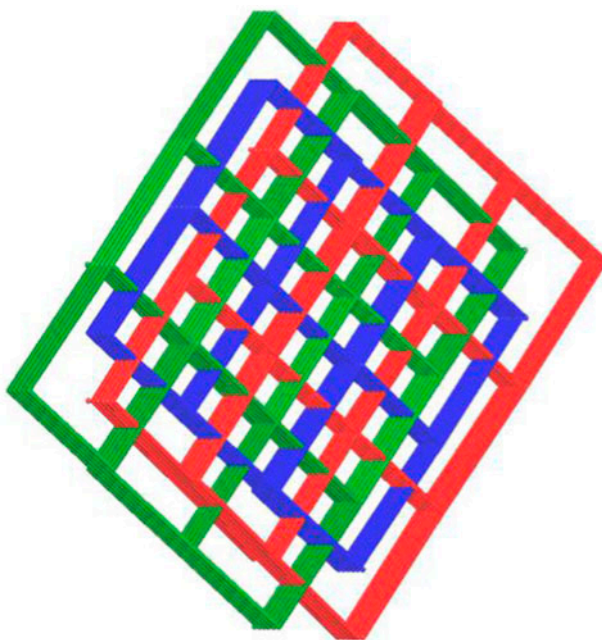


Figure 7. Schematic view showing the threefold interpenetrated 3-D topological network for **2**.

We compared our Mn(II) CPs to other Mn(II) CPs. Li and coworkers reported $\{[\text{Mn}(\text{bte})(\text{NO}_{2-1,3}\text{-bdc})(\text{H}_2\text{O})]\cdot\text{H}_2\text{O}\}_n$, $\{[\text{Mn}(\text{btp})(\text{NO}_{2-1,3}\text{-bdc})(\text{H}_2\text{O})]\cdot 2\text{H}_2\text{O}\}_n$ and $\{[\text{Mn}(\text{btb})(\text{NO}_{2-1,3}\text{-bdc})(\text{H}_2\text{O})]\cdot\text{H}_2\text{O}\}_n$ (bte, 1,2-bis(1,2,4-triazol-1-yl)ethane; btp, 1,3-bis(1,2,4-triazol-1-yl)propane; btb, 1,4-bis(1,2,4-triazol-1-yl)butane, $\text{NO}_{2-1,3}\text{-H}_2\text{bdc}$, 5-nitroisophthalic acid), which display 1-D \rightarrow 2-D interdigitated array and 2-D (4,4) network, respectively [26]. Chen and co-workers synthesized $[\text{Mn}(\text{aip})(\text{phen})]$ (H_2aip = 5-amino isophthalic acid and phen = 1,10-phenanthroline) with a 2-D layer structure [27]. Yang and co-workers reported $\{[\text{Mn}_3(\text{bpt})_2(\text{bib})_2(\text{H}_2\text{O})_2]\cdot(\text{H}_2\text{O})_2\}_n$ (H_3bpt = biphenyl-3,4',5'-tricarboxylic acid and bib = 1,4-bis(imidazolyl)benzene) with a 3-D wave-like zigzag structure [28]. Li and co-workers synthesized $[\text{Mn}(\text{dipt})(\text{m-BDC})_3]_n$ [dipt = 2-(2,4-dichlorophenyl)-1H-imidazo[4,5-f][1,10]-phenanthroline, m-BDC = isophthalic acid] with 1-D chain architecture [29]. Sun and co-workers reported $[\text{Mn}(\text{L})]$ and $[\text{Mn}(\text{L})(\text{pybim})]$ [H_2L = 5-(benzimidazol-1-ylmethyl)isophthalic acid, pybim = 2-(pyridin-2-yl)-1H-benzimidazole] with three-connected twofold interpenetrated 2-D network and a uninodal four-connected 2-D network with $(4^4\cdot 6^2)$ topology [30]. Zhang and co-workers synthesized $[\text{Mn}(\text{tda})(\text{ip})(\text{H}_2\text{O})]_n$ [H_2tda = thiophene-2,5-dicarboxylic acid, ip = 1H-imidazo-[4,5-f][1,10]-phenanthroline], showing a 2-D network and 3-D supramolecular structure through hydrogen bonding and $\pi\cdots\pi$ interactions [31].

3.2. Luminescent properties

The simulated and experimental XRPD pattern of **1** and **2** are given in figure S1 (see online supplemental material at <http://dx.doi.org/10.1080/00958972.2015.1021344>). The peak positions are in agreement with each other, indicating the phase purity of products.

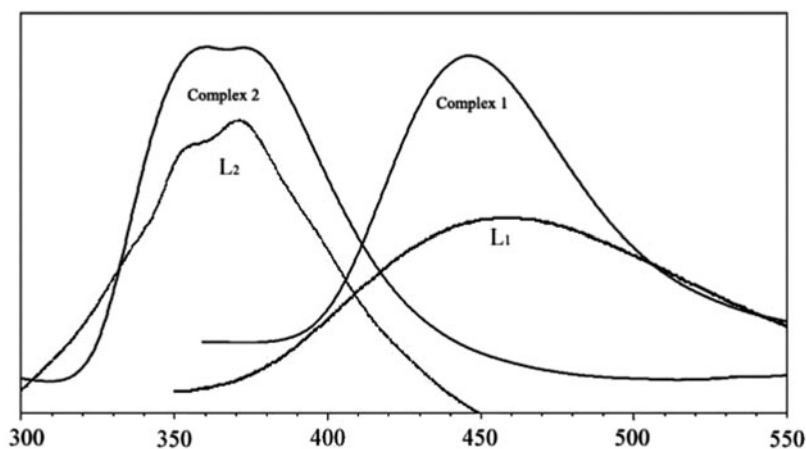


Figure 8. The luminescence spectra for **1** and **2** in the solid state at room temperature.

As depicted in figure 8, **1** and **2** exhibit fluorescent emission with maxima at 460 nm ($\lambda_{\text{ex}} = 350$ nm) for **1** and 365 nm ($\lambda_{\text{ex}} = 350$ nm) for **2**. Such fluorescence behavior may be attributed to the intraligand transition of coordinated nitrogen-containing ligands, since similar emissions at 456 nm ($\lambda_{\text{ex}} = 341$ nm), 348 and 361 nm ($\lambda_{\text{ex}} = 300$ nm) were observed for free L_1 and L_2 , respectively [32, 33]. The emission bands of the carboxylate ligands originated from the $\pi^* \rightarrow n$ transition are weak and the carboxylate ligands have no significant contribution to the fluorescence emission of **1** and **2** in the presence of the N-donor ligand [34].

4. Conclusion

We obtained two Mn(II) CPs based on 4,4'-sulfonyldicarboxylic acid, 1,4-bis(1-imidazolyl)benzene, and 4,4'-bis(1-imidazolyl)biphenylene ligands by the hydrothermal method. Complex **1** features a 2-D layer structure with sql topology and 1,4-bis(1-imidazolyl)benzene appears as non-coordinating molecule in structure as templates to construct **1**. Complex **2** shows a 3-D framework with the threefold interpenetrated CdS topological net.

Supplementary material

Crystallographic data for the structural analysis have been deposited with the Cambridge Crystallographic Data Center, CCDC reference numbers: 1001304 and 1001305. These data can be obtained free of charge at <http://www.ccdc.cam.ac.uk> (or Cambridge Crystallographic Data Center, 12 Union Road, Cambridge CB2 1EZ, UK; Fax: +44 1223 336 033; E-mail: deposit@ccdc.cam.ac.uk). Supplemental data for this article can be accessed <http://dx.doi.org/10.1080/00958972.2015.1021344>.

References

- [1] L.J. Murray, M. Dincă, J.R. Long. *Chem. Soc. Rev.*, **38**, 1294 (2009).
- [2] D.J. Tranchemontagne, K.S. Park, H. Furukawa, J. Eckert, C.B. Knobler, O.M. Yaghi. *J. Phys. Chem. C*, **116**, 13143 (2012).
- [3] Q.X. Jia, H. Tian, J.Y. Zhang, E.Q. Gao. *Chem. Eur. J.*, **17**, 1040 (2011).
- [4] J. Li, J. Tao, R.B. Huang, L.S. Zheng. *Inorg. Chem.*, **51**, 5988 (2012).
- [5] X.T. Zhang, D. Sun, B. Li, L.M. Fan, B. Li, P.H. Wei. *Cryst. Growth Des.*, **12**, 3845 (2012).
- [6] Y.J. Cui, Y.F. Yue, G.D. Qian, B.L. Chen. *Chem. Rev.*, **112**, 1126 (2012).
- [7] J. Qin, C. Qin, C.X. Wang, H. Li, L. Cui, T.T. Li, X.L. Wang. *CrystEngComm*, **12**, 4071 (2010).
- [8] L.Y. Wang, R.Q. Fan, P. Wang, Y.L. Yang. *Inorg. Chem. Commun.*, **23**, 54 (2012).
- [9] Y. Liu, M. Pan, Q.Y. Yang, L. Fu, K. Li, S.C. Wei, C.Y. Su. *Chem. Mater.*, **24**, 1954 (2012).
- [10] Z.P. Han, Y.H. Li. *Inorg. Chem. Commun.*, **22**, 73 (2012).
- [11] Y. Zhang, X. He, J. Zhang, P. Feng. *Cryst. Growth Des.*, **11**, 29 (2011).
- [12] X.L. Wang, C. Qin, E.B. Wang, Z.M. Su, L. Xu, S.R. Batten. *Chem. Commun.*, **48**, 4789 (2005).
- [13] L. Schlechte, V. Bon, R. Grönkler, N. Klein, I. Senkowska, S. Kaskel. *Polyhedron*, **44**, 179 (2012).
- [14] P.P. Cui, J.L. Wu, X.L. Zhao, D. Sun, L.L. Zhang, J. Guo, D.F. Sun. *Cryst. Growth Des.*, **11**, 5182 (2011).
- [15] R. Sen, D. Saha, S. Koner. *Chem. Eur. J.*, **18**, 5979 (2012).
- [16] Z.B. Zhu, W. Wan, Z.P. Deng, Z.Y. Ge, L.H. Huo, H. Zhao, S. Gao. *CrystEngComm*, **14**, 6675 (2012).
- [17] B.Y. Li, X.J. Zhou, Q. Zhou, G.H. Li, J. Hua, Y. Bi, Y.J. Li, Z. Shi, S.H. Feng. *CrystEngComm*, **13**, 4592 (2011).
- [18] J. Zhang, S.M. Chen, H. Valle, M. Wong, C. Austria, M. Cruz, X.H. Bu. *J. Am. Chem. Soc.*, **129**, 14168 (2007).
- [19] Z.Y. Lu, L.T. Du, B.S. Zheng, J.F. Bai, M.X. Zhang, R.R. Yun. *CrystEngComm*, **15**, 9348 (2013).
- [20] Q.X. Yang, X.Q. Chen, Z.J. Chen, Y. Hao, Y.Z. Li, Q.Y. Lu, H.G. Zheng. *Chem. Commun.*, **48**, 10016 (2012).
- [21] Y. Qi, F. Luo, Y.X. Che, J.M. Zheng. *Cryst. Growth Des.*, **8**, 606 (2008).
- [22] F. Guo, B.Y. Zhu, M.L. Liu, X.L. Zhang, J. Zhang, J.P. Zhao. *CrystEngComm*, **15**, 6191 (2013).
- [23] F. Guo, B.Y. Zhu, G.L. Xu, M.M. Zhang, X.L. Zhang, J. Zhang. *J. Solid State Chem.*, **199**, 42 (2013).
- [24] *SAINT Software Reference Manual*, Bruker AXS, Madison, WI (1998).
- [25] G.M. Sheldrick. *SHELXTL NT, Version 5.1, Program for Solution and Refinement of Crystal Structures*, University of Göttingen, Göttingen (1997).
- [26] X. Zhu, S. Zhao, Y.F. Peng, B.L. Li, H.Y. Li. *J. Coord. Chem.*, **67**, 1317 (2014).
- [27] J.J. Wang, Q.L. Bao, J.X. Chen. *J. Coord. Chem.*, **66**, 2578 (2013).
- [28] Y.L. Lu, W.J. Zhao, X. Feng, Y. Chai, Z. Wu, X.W. Yang. *J. Coord. Chem.*, **66**, 473 (2013).
- [29] Y. Li, C.B. Li. *J. Coord. Chem.*, **65**, 4288 (2012).
- [30] H.W. Kuai, T.A. Okamura, W.Y. Sun. *J. Coord. Chem.*, **65**, 3147 (2012).
- [31] X.L. Zhang, K. Cheng. *J. Coord. Chem.*, **65**, 3019 (2012).
- [32] H.J. Cheng, H.X. Li, Z.G. Ren, C.N. Lü, J. Shi, J.P. Lang. *CrystEngComm*, **14**, 6064 (2012).
- [33] G.L. Xu, F. Guo. *Inorg. Chem. Commun.*, **27**, 146 (2013).
- [34] Y.W. Li, H. Ma, Y.Q. Chen, K.H. He, Z.X. Li, X.H. Bu. *Cryst. Growth Des.*, **12**, 189 (2012).